Schlieren imaging with fractional Fourier transform to visualise ultrasonic fields

Tim Hetkämper, Leander Claes, Bernd Henning
Measurement Engineering Group, Paderborn University, Warburger Straße 100, 33098 Paderborn, Germany,
hetkaemper@emt.uni-paderborn.de

Abstract

Schlieren imaging is widely used to visualise local density modulations in optically transparent media, for example to make fluid flow or ultrasonic waves visible. In common schlieren setups, spatial filtering is applied. This is accomplished by a $2f$-arrangement consisting of two lenses, where f is the focal length of the used lenses. Between the lenses, a spatial filter is positioned. The filter requires precise adjustment to obtain images showing the ultrasonic waves. In this paper a method is described to visualise ultrasonic fields that does not require spatial filtering. To accomplish this, a focussing macro lens is used. The observed effects are in accordance with the theory of the fractional Fourier transform.

1 Introduction

A common method to visualise local density modulations in optically transparent media is schlieren imaging. This enables the visualisation of fluid flow or ultrasonic waves and the investigation of physical phenomena such as reflection and transmission of ultrasonic waves. Moreover, schlieren imaging is often used to visualise the sound field of ultrasonic transducers. In practical applications, transducers are often driven in burst mode. Thus it is of interest to visualise the propagating waves in time and space. A pulsed illumination source and the excitation of the ultrasonic transducer are synchronised employing the stroboscopic principle. By varying the delay between the two trigger signals, images of different wave positions can be obtained.

An advantage of schlieren imaging compared to hydrophone measurements is that the sound field is not disturbed by a sensor. Moreover, the measurement time is lower, as a single schlieren image contains many pixels, whereas hydrophone measurements require scanning the field by physically moving the sensor to every single measurement point.

In the following section a classical schlieren setup is described, which requires a spatial filter that needs precise adjustment. As explained in section 3, ultrasonic waves can be visualised without applying a filter. This is accomplished by varying the position of a lens. The observations are in accordance with the theory of the fractional Fourier transform and mathematically verified by a simulated signal in section 4. Finally, the procedure to reconstruct a representation of the phase object from recorded images is described.

2 Schlieren imaging

Schlieren imaging relies upon the interaction of an ultrasonic wave with an electromagnetic wave. An ultrasonic wave with wavelength λ_{US} which propagates through a medium constitutes a local pressure and density modulation. Due to the piezo-optic effect, also the refractive index of the medium is modulated. If the medium is illuminated with a plane electromagnetic wave E_0 with wavelength λ_0, a spatially dependent phase shift occurs in the wavefronts [1], see Figure 1. When observing ultrasonic waves, these phase shifts are usually small and a so-called weak phase object is obtained. This indicates there are no changes in amplitude and no deflection in the sense of geometrical optics. The phase object can be described via the transmission function [2]

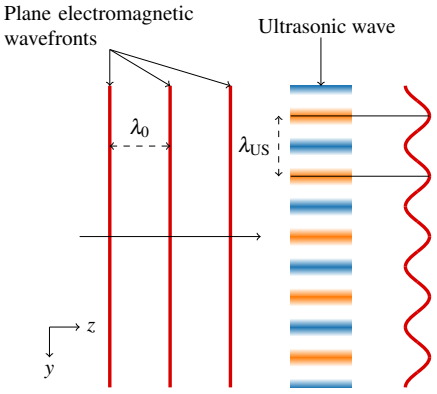

Figure 1 Phase shift in plane electromagnetic waves caused by an ultrasonic wave.

$$t(x,y) = e^{j\varphi(x,y)} , \tag{1}$$

which due to $|\varphi| \ll 1$ can be approximated by

$$t(x,y) = 1 + j\varphi(x,y) . \tag{2}$$

A typical setup for recording schlieren images is shown in Figure 2. Laser radiation with a wavelength of $\lambda_0 = 662\,\text{nm}$ passes through a microscope objective creating a divergent beam. A pinhole is placed at the focus of the microscope objective to remove disturbances of the wavefront by e.g.

ISBN 978-3-8007-5835-7

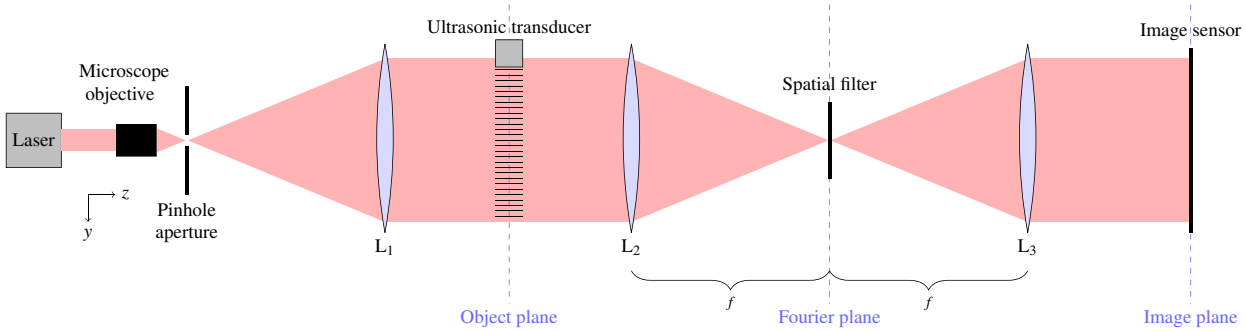

Figure 2 Typical setup for recording schlieren images.

diffraction at dust particles [3]. Lens L_1 collimates the beam.

The so-called object plane, where an ultrasonic transducer is located, is thus illuminated by the plane electromagnetic wave E_0. The ultrasonic transducer is placed in a water basin (not shown) and emits ultrasonic waves. With the transmission function (Equation 2), the electromagnetic field in the object plane $E_{\mathrm{OP}}(x,y)$ is described by

$$E_{\mathrm{OP}}(x,y) = E_0 \cdot t(x,y)\ . \tag{3}$$

The schlieren image is recorded by a digital camera with an image sensor. An image sensor can only detect the intensity $I(x,y)$, i. e. the square of the absolute value of the incident electromagnetic radiation:

$$I(x,y) = |E(x,y)|^2\ . \tag{4}$$

Thus, phase information is lost and phase objects cannot be observed directly. Therefore, spatial filtering is applied in common schlieren setups. This is accomplished by a $2f$-arrangement consisting of two additional lenses. Lens L_2 is used to realise a spatial Fourier transform [4]: At a distance of the focal length f, the Fourier transform of the object plane can be observed in the so-called Fourier plane:

$$E_{\mathrm{FP}}(k_x,k_y) = \mathscr{F}\{E_{\mathrm{OP}}(x,y)\} \tag{5}$$

with k_x, k_y being the wavenumbers with respect to x, y. By placing optical filters in the Fourier plane, spatial filtering can be performed [3]. The transmission characteristic of the filter is described by the filter function $F_{\mathrm{F}}(k_x,k_y)$. Another lens L_3 is placed at a distance of f from the Fourier plane, realising the inverse Fourier transform. Accordingly, the electromagnetic radiation in the image plane equates to

$$\begin{aligned} E_{\mathrm{IP}}(x,y) &= \mathscr{F}^{-1}\{E_{\mathrm{FP}}(k_x,k_y)\cdot F_{\mathrm{F}}(k_x,k_y)\} &(6)\\ &= \mathscr{F}^{-1}\{\mathscr{F}\{E_{\mathrm{OP}}(x,y)\}\cdot F_{\mathrm{F}}(k_x,k_y)\}\ . &(7)\end{aligned}$$

Depending on the used spatial filter, different representations of the phase object become visible on the image sensor. An optical high-pass filter is often used, which blocks wavenumbers near $k_x, k_y = 0$. A schlieren image recorded with a high-pass filter is shown in Figure 3. At the top of the image, the outline of the transducer is visible. The transducer *Panametrics V303* is excited at its resonance frequency of 1 MHz with a sine burst of 10 cycles and an amplitude of 32 V. As according to Equation 4 the image sensor can only observe the intensity $I(x,y)$, sign information is lost. Hence no differentiation between minima and maxima of the sound pressure is possible.

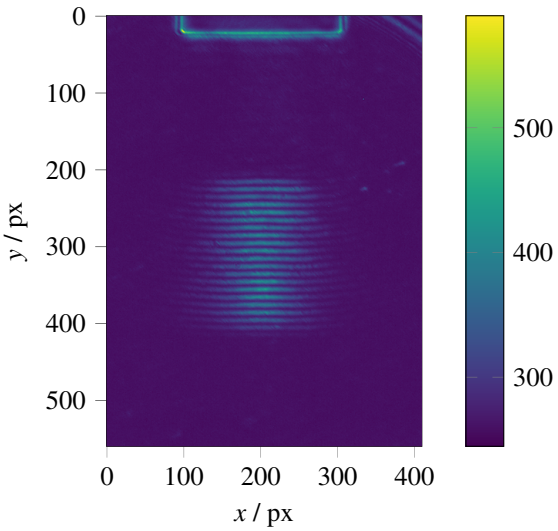

Figure 3 Typical schlieren image. The transducer *Panametrics V303* is excited at its resonance frequency of 1 MHz with a sine burst of 10 cycles and an amplitude of 32 V. The values are raw values of a 12-bit image sensor.

3 Fractional Fourier transform

In the schlieren setup deployed at the Measurement Engineering Group, a standard digital camera equipped with a macro lens is used to record the images (represented by L_3 and the image sensor in Figure 2). The macro lens has a fixed focal length but the focus is adjustable. Adjusting the focus corresponds to moving L_3 on the z-axis.

To be able to apply spatial filtering, the focus is adjusted to invert the Fourier transform (L_3 at distance f to Fourier plane, see Figure 2). In the following this setting is referred to as *focussed*. Mathematically, applying no filter corresponds to $F_{\mathrm{F}}(k_x,k_y) = 1$, so Equation 7 equates to

$$\begin{aligned} E_{\mathrm{IP}}(x,y) &= \mathscr{F}^{-1}\{\mathscr{F}\{E_{\mathrm{OP}}(x,y)\}\} &(8)\\ &= E_{\mathrm{OP}}(x,y)\ . &(9)\end{aligned}$$

As described by Equation 4, the image sensor cannot detect

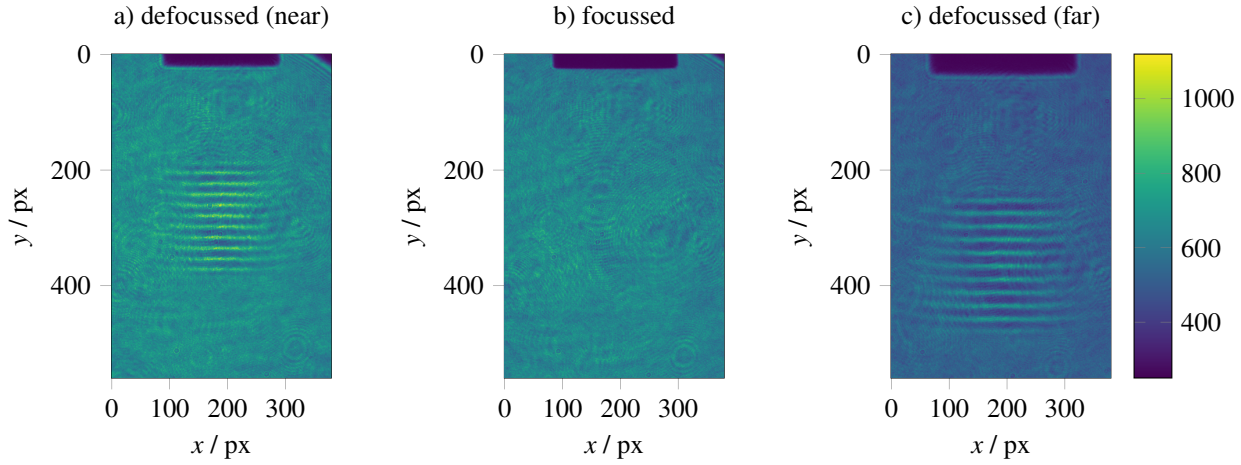

Figure 4 Images recorded without spatial filter and different focus settings. Transducer and excitation signal are the same as in Figure 3. The values represent raw values of a 12-bit image sensor. Note that the size of the observed object changes with varying focus.

the phase of the incident electromagnetic radiation. Consequently when no spatial filter is applied only a uniformly lit area can be observed (see Figure 4b). At the top of the image the outline of the transducer is visible as it is opaque to visible light. Note that due to non-idealities of the optical components some interference patterns are visible.

If the focus is adjusted, a non-integer Fourier transform is performed. This can be described mathematically via the fractional Fourier transform $\mathscr{F}^a$ with the order a. It is defined as [5]

$$\mathscr{F}^a\{g(y)\} = \int_{-\infty}^{\infty} g(y) \cdot K_a(y', y)\,\mathrm{d}y \tag{10}$$

with the transform kernel

$$K_a(y', y) = A_\alpha \mathrm{e}^{\mathrm{j}\pi(\cot(\alpha)y'^2 - 2\csc(\alpha)y'y + \cot(\alpha)y^2)} \tag{11}$$

where

$$A_\alpha = \sqrt{1 - \mathrm{j}\cot(\alpha)} \tag{12}$$

and α is the order a expressed as angle

$$\alpha = a\pi/2\,. \tag{13}$$

For clarity reasons only the one-dimensional formulation in the propagation direction y of the ultrasonic wave is shown here. An order of $a = 0$ corresponds to the original signal

$$\mathscr{F}^0\{g(y)\} = g(y)\,, \tag{14}$$

whereas an order of $a = 1$ corresponds to the Fourier transform

$$\mathscr{F}^1\{g(y)\} = \mathscr{F}\{g(y)\}\,. \tag{15}$$

$\mathscr{F}^2$ mirrors the original signal

$$\mathscr{F}^2\{g(y)\} = g(-y) \tag{16}$$

and $\mathscr{F}^3$ yields the mirrored Fourier transformed signal, which corresponds to performing an inverse Fourier transform:

$$\mathscr{F}^3\{g(y)\} = \mathscr{F}^1\{g(-y)\} = \mathscr{F}^{-1}\{g(y)\}\,. \tag{17}$$

$\mathscr{F}^4$ yields the original signal, as the fractional Fourier transform is periodic in a with a periodicity of 4.

If the setup is slightly defocussed (moving L_3 nearer to the Fourier plane), a representation of the phase object can be observed (Figure 4a). An oscillation is visible with values lower (blue) and higher (yellow) than the background illumination. This corresponds to performing less than a full inversion of the Fourier transform, i. e. instead of Equation 8 the signal in the image plane is given by

$$E_{\mathrm{IP}}(x,y) = \mathscr{F}^{-1+b}\{\mathscr{F}^1\{E_{\mathrm{OP}}(x,y)\}\} \tag{18}$$

$$= \mathscr{F}^b\{E_{\mathrm{OP}}(x,y)\} \tag{19}$$

with $b > 0$. If the focus is adjusted in the opposite direction (moving L_3 farer away from the Fourier plane), Equation 19 also applies, but now with $b < 0$. As depicted in Figure 4c, a representation of the phase object can also be observed.

Note that varying the focus also changes the size of the observed object on the image sensor. It is apparent that the size of the transducer increases from Figure 4a to c. A larger size also implies the electromagnetic radiation extends to a larger area. As the images are all recorded with equal camera and illumination settings, this is why the background intensity decreases from Figure 4a to c.

4 Verification with simulated signals

To verify the observations mathematically, a one-dimensional signal is regarded. Figure 5 shows the transmission function $t(y)$ of a phase object in the object plane, which is a sine-burst modulated with a Hann window. The sine wave has a wavelength of $\lambda_{\mathrm{US}} \approx 1.5\,\mathrm{mm}$. As no modification of the amplitude is performed, the absolute value $|t(y)|$ is constant while the phase $\arg(t(y))$ is oscillating.

To simulate the recording of images with different focus settings, the transmission object is fractionally Fourier transformed [6] for orders $a = 0.03$ and $a = -0.03$. The absolute value of the obtained signals is depicted in Figure 6.

ISBN 978-3-8007-5835-7

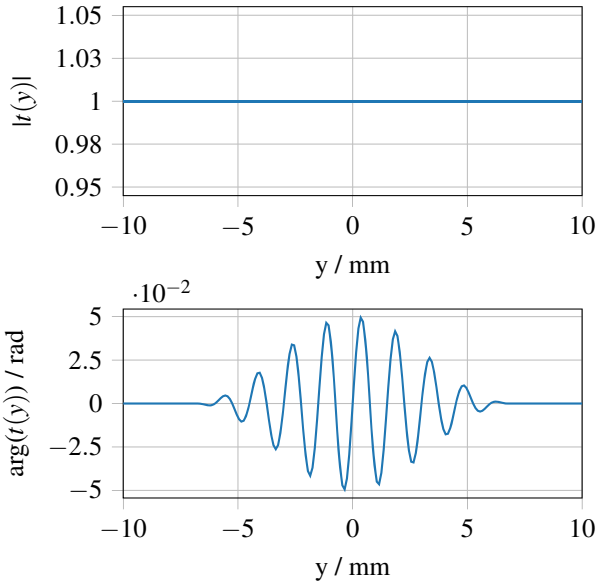

Figure 5 Transmission function $t(y)$ of a phase object in the object plane.

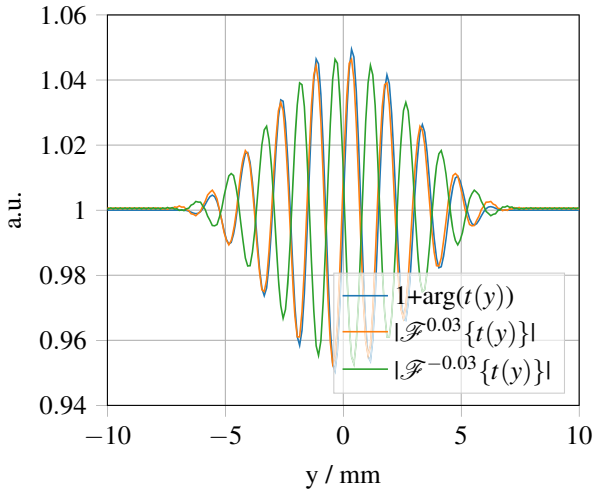

Figure 6 Absolute value of the fractional Fourier transforms of the transmission function $t(y)$ shown in Figure 5 compared to the phase $\arg(t(y))$ offset by 1.

Compared to Figure 5, the absolute value of 1 is superimposed by an oscillation. To be able to draw a comparison to the phase $\arg(t(y))$, an offset of 1 is added to $\arg(t(y))$ and additionally depicted in Figure 6. The oscillation of the absolute value of both fractional Fourier transforms is in good agreement with $1+\arg(t(y))$. As expected, the signal with the negative order $a=-0.03$ is inverted to the one with the positive order $a=0.03$.

5 Image postprocessing

The images shown in Figure 4 all have a background illumination and show artifacts caused by non-ideal optical components. To reconstruct the oscillation, the following procedure is used: First of all, the square root is applied to the recorded image's values P_{US}. This inverts the square caused by recording the intensity (Equation 4). To reduce artifacts, a reference image P_{ref} without transmitting an ultrasonic wave is recorded and subtracted from the image with the ultrasonic wave present:

$$P_{\mathrm{osc}} = \sqrt{P_{\mathrm{US}}} - \sqrt{P_{\mathrm{ref}}}\,. \tag{20}$$

Moreover, a Gaussian filter is applied to reduce noise. The resulting image P_{osc} is depicted in Figure 7. A vertical slice at $x=200$ px is shown in Figure 8. As can be observed in both figures, P_{osc} contains sign information and thus can be used for further analysis, e.g. for tomographic reconstruction, if multiple images at different transducer angles are recorded [7].

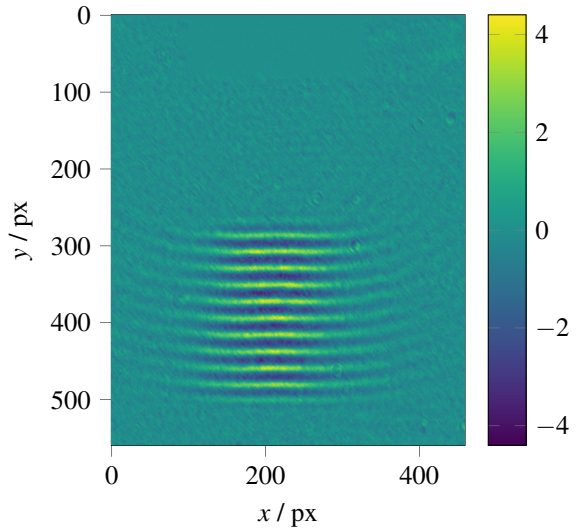

Figure 7 Image P_{osc} postprocessed according to Equation 20.

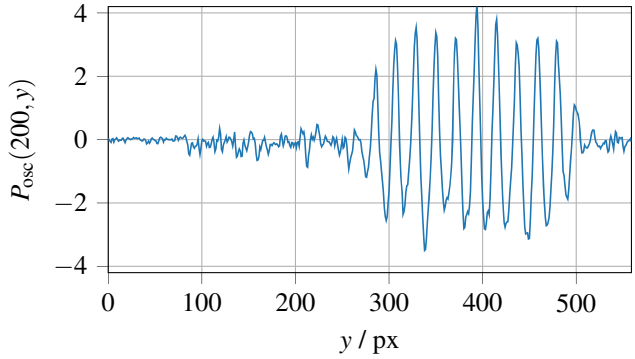

Figure 8 Vertical slice at $x=200$ px of the postprocessed image P_{osc} shown in Figure 7.

6 Conclusion

This work presents a method to record schlieren images without the need of a spatial filter. Through varying the focus distance, a fractional Fourier transform of the incident

ISBN 978-3-8007-5835-7

electromagnetic radiation is performed. This shifts information from the phase to the absolute value of the electromagnetic field, which makes the schlieren object visible to a camera. Only small changes of the focus are necessary, which translates to small fractional Fourier transform orders $a \ll 1$. Regarding Equation 19, this could allow to shorten the length of schlieren measurement setups, as the space required to perform a full optical Fourier transform and corresponding inverse transform is no longer needed.

7 Literature

[1] Raman, C.V.; Nagendra Nath, N.S.: The diffraction of light by high frequency sound waves: Part I. Proc. Indian Acad. Sci. 2 (1935), pp. 406–412.

[2] Stößel, W.: Fourieroptik – Eine Einführung. Berlin Heidelberg: Springer-Verlag, 1993.

[3] Lauterborn, W.; Kurz, T.: Coherent Optics – Fundamentals and Applications. 2nd Ed. Berlin Heidelberg: Springer-Verlag, 2003.

[4] Goodman, J.W.: Introduction to Fourier Optics. 3rd edition. Englewood: Roberts & Company Publishers, 2005.

[5] Ozaktas, H.M.; Zalevsky, Z.; Kutay, M.A.: The fractional Fourier transform with applications in optics and signal processing. Chichester: Wiley, 2001.

[6] Ozaktas, H.M.; Kutay, M.A.; Bozdagi, G.: Digital computation of the fractional Fourier transform. IEEE Trans. Sig. Proc. 44 (1996), pp. 2141–2150.

[7] Hetkämper, T.; Dreiling, D.; Claes, L.; Henning, B.: Tomographie des Schallfelds von Ultraschallwandlern mittels Schlierentechnik. Fortschritte der Akustik – DAGA 2021, pp. 1520–1523.

ISBN 978-3-8007-5835-7